Tuning of oscillation modes by controlling dimensionality of spin structures

Authors: Hee-Sung Han[1,2], Sooseok Lee[2], Min-Seung Jung[3], Namkyu Kim[2], Dae-Han Jung[2], Myeonghwan Kang[2], Hye-Jin Ok[2], Weilun Chao[1], Young-Sang Yu[4,5], Jung-Il Hong[3], Mi-Young Im[1]*, and Ki-Suk Lee[2]*

Affiliations:

[1]Center for X-ray Optics, Lawrence Berkeley National Laboratory, Berkeley, CA, 94720, USA

[2]Department of Materials Science and Engineering, Ulsan National Institute of Science and Technology (UNIST), Ulsan, 44919, Republic of Korea

[3]Department of Emerging Materials Science, Daegu Gyeongbuk Institute of Science and Technology (DGIST), Daegu 42988, Republic of Korea

[4]Advanced Light Source, Lawrence Berkeley National Laboratory, Berkeley, CA, 94720, USA

[5]Department of Physics, Chungbuk National University, Cheongju 28644, Republic of Korea

[*]Correspondence to Mi-Young Im (email: mim@lbl.gov) and Ki-Suk Lee (email: kisuk@unist.ac.kr).

Abstract

Harmonic oscillation of spin structures is a physical phenomenon that offers great potential for applications in nanotechnologies such as nano-oscillators and bio-inspired computing. The effective tuning of oscillations over wide frequency ranges within a single ferromagnetic nanoelement is a prerequisite to realize oscillation-based nanodevices, but it has not been addressed experimentally or theoretically. Here, utilizing a vortex core structure, one of spin structures, we report a drastic change of oscillation modes over the frequency range from MHz to sub-GHz in a 100 nm-thick permalloy circular disk. Oscillation mode was found to considerably depend on the shape and dimension of the vortex core structure and various oscillation modes over a wide range of frequencies appeared with dimensional change in the vortex core structure. This work demonstrates that oscillation modes of the vortex core structure can be effectively tuned and opens a way to apply spin structures to oscillation-based technology.

Keywords: Spintronics, Nano-oscillator, Oscillation modes, Spin dynamics, X-ray microscopy, Magnetic vortex.

Introduction

Harmonic oscillation is an intriguing physical phenomenon that has attracted significant attentions in various material systems. The fundamental understanding and manipulation of oscillation properties (e.g., frequency and amplitude) have been extensively studied in the research fields of two-dimensional (2D) materials[1-3], quantum materials[4,5], lattice distortion[6,7] and magnetic materials[8-10] since it offers a high potential for energy-efficient technological applications, e.g., nano-oscillators[1,2,11-13], bio-inspired computing[5,14-18], and programmable logic devices[19,20].

Spin structures have been highly regarded in the application to oscillation-based nanodevices due to its high stability and rich oscillation properties[21-28]. The magnetic vortex, one of spin structures, is a ground state stabilized in a soft ferromagnetic disk, which is composed of the in-plane curling magnetization and out-of-plane magnetization at the centre of the element, referred to as a vortex core. The vortex core structure in typical thin ferromagnetic disks where the thickness is within the range of the exchange length (thickness < 50 nm) is considered as a rigid structure and it generally shows the gyrotropic motion of the MHz-ranged frequency without its deformation along the thickness direction, which is called the zeroth-order gyrotropic mode[29-32]. The oscillation mode of vortex core structure can be easily detected through the electrical measurements compared to the oscillation mode of other spin structures due to its large amplitude and narrow linewidth[11-13]. Recently, it has been

revealed that the oscillation mode could significantly change as the thickness of the disk increases and it leads to the emergence of unique three-dimensional (3D) dynamic characteristics of magnetic vortex[33-41]. For instance, the higher-order gyrotropic modes with GHz frequency range accompanying oscillation nodes along the thickness of the disk appear in addition to zeroth-order gyrotropic modes[38-41].

To realize a versatile nano-oscillator, efficient tuning of harmonic oscillations of vortex core structure in a wide range of frequencies, especially in a single ferromagnetic element is highly required[31,42,43]. However, earlier works on the oscillation of vortex core structure have focused on tuning the eigenfrequency of the zeroth-order gyrotropic mode of vortex core structure in thin ferromagnetic disks, and thus the reported frequency tuning range has been limited to MHz range[31,42,43]. In our works, we manipulate oscillation modes of vortex core structure over from MHz to sub-GHz frequency range within a 100 nm-thick single permalloy ($Ni_{80}Fe_{20}$, Py) circular disk utilizing time-resolved magnetic transmission X-ray microscopy (MTXM) measurement (Figure 1a). We show that the oscillation modes of the vortex core structure are controllable by manipulating the shape and dimension of the vortex core structure.

Results

Manipulating the shape and dimension of the vortex core structure

Figure 1b shows three different magnetic structures imaged at the external magnetic fields of H_x = 0 mT, 12 mT, and 24 mT in permalloy ($Ni_{80}Fe_{20}$, Py) circular disk of diameter D = 3 μm and thickness h = 100 nm by utilizing MTXM (See Methods)[44]. Black and white contrasts in those images indicate downward and upward magnetic components, respectively. At zero field (H_x = 0 mT), a black spot at the centre of the disk is observed, which corresponds to the typical dot-shaped vortex core structure with downward magnetization. As H_x increase to +12 mT, the vortex core structure is shifted in the +y-axis and the vortex core structure gets slightly enlarged in a horizontal direction. As H_x increases further, the vortex core structure gets closer to the edge of the disk and completely deforms into the elongated structure with curvature (See the magnetic image at H_x = +24 mT in Figure 1b). The magnetic images in Figure 1b show that the shape and dimension of the vortex core structure noticeably change as it gets closer to the edge of the disk by increasing the external magnetic field (See zoomed images). Figure 1c indicates the simulated magnetic structures (See Methods)[45], which match well with the experimentally observed structures.

The detailed 3D magnetization configurations of vortex core structures (marked by the yellow dashed box in Figure 1c) are displayed in Figure 1d. The volumes of vortex core structures with $m_z \leq -0.8$ are indicated by blue colour. One can see that as the field varies, the shape of the vortex core structure changes and the vortex core structure is transformed from a one-dimensional (1D) vortex core structure to a 2D vortex core structure containing a

domain wall. At H_x = 0 mT, a typical 1D vortex core structure (hereafter, called VC_1 structure) is observed; the vortex cores on the top and bottom surfaces are coaxially aligned, which supports that the VC_1 structure is a 1D vortex core structure (See orange dotted arrow). In the vortex core structure at H_x = 12 mT (hereafter, called VC_2 structure), the vortex cores on top and bottom surfaces are still coaxially aligned like VC_1 structure, which supports that VC_2 structure is also a 1D structure (See orange dotted arrow). However, unlike VC_1 structure, the shape of VC_2 structure is slightly expanded along the horizontal direction and the magnetization of the VC_2 structure is not completely uniform along the thickness of the disk, which might occur to compensate for the demagnetization energy induced by the vortex core structure shifting toward the edge of the disk. At H_x = 24 mT, the vortex core structure (hereafter, called VC_3 structure) is largely deformed. The vortex cores located on the top and bottom surfaces of the disk are no longer coaxial and the two vortex cores on the top and bottom surfaces of the disk are connected through the domain wall stretched along the *x*-axis (See Supplementary Figure 1 and Supplementary Note 1), which indicates that the VC_3 structure is clearly a 2D vortex core structure (See orange dotted arrows)[21,40,46-51]. We confirmed that the dimensional change of the vortex core structure starts occurring at H_x = 15 mT, and the domain wall connecting the vortex cores on the top and bottom surfaces of the disk gets longer as H_x increases until the vortex core structure is annihilated at H_x = 62 mT (See Supplementary Figure 2 and Supplementary Note 2). Additionally, it was confirmed that

the dimensional change of vortex core structure by applying magnetic field only occurs when the disk is thicker than or equal to 70 nm in the Py circular disk of D = 3 μm (See Supplementary Figure 2 and Supplementary Note 2). It is noticed that the observed dimensional change of vortex core structure is analogous to the one achieved by changing the geometry of the disk from square to the rectangle[51]. The results in Figure 1 demonstrate that the shape and dimension of vortex core structure in thick ferromagnetic disks can be controlled simply by applying in-plane magnetic fields.

Dynamics of 1D vortex core structures

To investigate the oscillation mode of vortex core structures formed with varying external magnetic fields, we performed time-resolved MTXM measurements[44] (See Methods). To excite the dynamic motions of the vortex core structures, we injected the magnetic field pulse with an amplitude of 1 mT and a pulse width of 1.12 ns to the disk along the $-x$-axis. Figures 2a and 2b show the representative snapshots of the dynamic motions of VC_1 and VC_2 structures, respectively. To track the position of vortex core structures, we defined area A of the vortex core structure with the normalized MTXM contrast less than 0.2 as denoted by the red closed curves (See Figure 2c and Methods). Both vortex core structures show the clockwise (CW) gyrotropic motion (See Figures 2a, 2b, Supplementary Movies 1, 2, and Supplementary Figure 3). However, the shapes of the two vortex core structures

become distinct from each other during their dynamic motions. The shape of the VC_2 structure, indicated by the red closed curves in Figure 2b, is varied from (to) circular to (from) elliptical shape during its dynamic motion, whereas the shape of the VC_1 structure stays the same, circular shape over the dynamic process. To quantitatively analyse the change of shape and size of those vortex core structures, we measured the variation of A (ΔA) during their dynamic motions. Figure 2d clearly shows that unlike the case of the VC_1 structure showing subtle random fluctuations, ΔA of the VC_2 structure is largely and periodically varied during its dynamic motion. It should be noticed that the noticeable changes of shape and size have never been reported in the dynamic motion of vortex core structures in typical thin ferromagnetic disks[22,23].

For deeper understanding of the shape and size variation of the VC_2 structure, we performed micromagnetic simulations for the dynamic motions of both VC_1 and VC_2 structures (See Methods). Figures 2e and 2f illustrate the simulated magnetization images during the dynamic motions of VC_1 and VC_2 structures, respectively. The shape and size of the VC_2 structure noticeably change during the dynamic motion as observed in experiments unlike those of the VC_1 structure (Figures 2e, 2f, Supplementary Movies 3 and 4). Detailed 3D magnetization configurations of VC_1 and VC_2 structures during their dynamic motions were investigated to clearly interpret the change of shape and size of the VC_2 structure seen in 2D images, respectively (Figures 2e and 2f). The respective trajectory curves of vortex core

motions on the top and bottom surfaces of the disk are added. For the VC_1 structure, the gyrotropic motions with circular trajectories are observed in both vortex cores on the top and bottom surfaces. In the VC_2 structure, however, vortex cores show the gyrotropic motions with elliptical trajectories. Interestingly, the major axis of the elliptical trajectories observed in the VC_2 structure is aligned to the axis rotated by an angle of $|\theta| \sim 35°$ with respect to the magnetic field pulse direction (x-axis, $|\theta| = 0°$) , which is in sharp contrast to previous reports that the major axis of the elliptical trajectory of vortex core gyrotropic motion in off-resonance is aligned to be parallel (x-axis, $|\theta| = 0°$) or perpendicular (y-axis, $|\theta| = 90°$) to the magnetic field pulse direction (x-axis, $|\theta| = 0°$)[31,32]. More importantly, the directions of major axes of the elliptical trajectories of vortex core motions on the top and bottom surfaces are not aligned. The major axis of the elliptical trajectories of the vortex cores of the top and bottom surfaces are aligned to the axis rotated by $\theta = -35°$ and $\theta = +35°$, respectively.

It is worth noting that the vortex core on the top surface is slightly lagging behind that on the bottom surface in both VC_1 and VC_2 structure, which indicates that there is a phase difference in the gyrotropic motions of the vortex cores of the top and bottom surfaces (Figure 2g). The non-zero phase difference of the gyrotropic motions of vortex cores on the top and bottom surfaces causes structural strain of the vortex core structure and is reflected as a slightly inclined structure in the thickness direction.[34] We estimated the phase differences of the gyrotropic motions of vortex cores on the top and bottom surfaces $\Delta\delta$ during the dynamic

motion of VC_1 and VC_2 structures (Figure 2h). In the VC_1 structure, the $\Delta\delta$ occurred between the two vortex cores on the top and bottom surfaces remains the same over the dynamic motion (blue line in Figure 2h). Surprisingly, $\Delta\delta$ in VC_2 structure is periodically varied during the dynamic motion of the VC_2 structure (red line in Figure 2h), which is probably due to the different directions of major axes of the elliptical trajectories of the vortex cores on the top and bottom surfaces (See Supplementary Movie 5). Based on the simulations results (Figures 2e-2h), it can be understood that the shape and size of VC_1 structure rarely varied (Figures 2a and 2d) due to the $\Delta\delta$ remaining constant in the structure (Figure 2h). On the other hand, the variation of the $\Delta\delta$ of the VC_2 structure (Figure 2h) causes the periodic shape change of the VC_2 structure from (to) circular to (from) elliptical shape as shown in Figures 2b and 2d.

Dynamics of the 2D vortex core structure

Figure 3 shows the dynamic motion of the VC_3 structure, which is significantly different from those of VC_1 and VC_2 structures (See Figure 3a and Supplementary Movie 6). The flexure oscillation of the VC_3 structure with the lateral motion and severe shape deformation is witnessed as shown in Figure 3a. The position and shape changes of the VC_3 structure during its dynamic motion are clearly observed as seen in green areas (right panel of Figure 3a). In Figure 3, the black and red curves represent the initial position of the VC_3

structure at t = 0 ns and its perturbed position triggered by the same magnetic field pulse applied to VC_1 and VC_2 structures.

Figure 3b displays the simulated magnetization image of the VC_3 structure and 3D magnetization configurations during the dynamic motion. It is noticed that the domain wall portion of the VC_3 structure shows the flexure oscillation as well as the lateral motion clearly visualized in experimental results (Figure 3a). It expands and shrinks repetitively in the horizontal direction (See Supplementary Movie 7). We traced the change of green areas in Figure 3a and 3b to quantitatively estimate the position change of the VC_3 structure (Figure 3c) and found that the position of the VC_3 structure was largely fluctuated (Figure 3c) after the initial lateral motions triggered by magnetic field pulse injected.

Our micromagnetic simulation verified that while the domain wall portion of the VC_3 structure experiences the flexure oscillation with the rigorous lateral motion (Figure 3b), the vortex cores on the top and bottom surfaces of the disk still show gyrotropic motions similar to those of VC_1 and VC_2 structures (Figure 3d). Figure 3d exhibits that the trajectory of the vortex core motions on the top and bottom surfaces (VC^{Top} and VC^{Bot}) are elliptical as observed in the dynamic motion of the VC_2 structure. However, vortex cores on the top and bottom surfaces of the VC_3 structure show not only the phase difference but also considerably different gyrotropic radius. Those differences of phase and gyrotropic radius of vortex cores on the top and bottom surfaces that occurred during the dynamic motion of the VC_3 structure

might be responsible for the flexure oscillation and shape deformation of the domain wall connecting the two cores on surfaces. As the dimension of the vortex core structure changes from 1D to 2D, the dynamic motion of the vortex core structure becomes more complex with the oscillation of the domain wall in addition to the gyrotropic motions of vortex cores on surfaces.

Oscillation modes of vortex core structures with different dimensions.

To investigate oscillation modes of 1D and 2D vortex core structures, we obtained the fast Fourier transformation (FFT) power spectra for the VC_1 and VC_3 structures taken from MTXM measurements (Figure 4a and Methods). The peak in FFT power spectra indicates an individual oscillation mode of vortex core structures. The blue and red lines in Figure 4a indicate the FFT power spectrum for the VC_1 and VC_3 structures. It clearly indicates the frequency of oscillation modes of 1D vortex core structures is different from those of 2D vortex core structures. Moreover, the number of peak increases in the frequency range from MHz to sub-GHz as the dimension of the vortex core structure changes from 1D to 2D indicating that the dimensional change of the vortex core structures leads to the emergence of the oscillation modes with sub-GHz frequency. To corroborate the experimental observation, we performed micromagnetic simulation (Figure 4b and Methods). Figure 4b shows FFT power spectra for the vortex core structures with varying H_x, obtained

from the micromagnetic simulation. Each branch in FFT power spectra indicates an individual oscillation mode of vortex core structures. The frequencies of two oscillation modes in the low field region (H_x < 12 mT) where VC_1 structure is stabilized, are rarely changed. However, at 12 mT ≤ H_x < 15 mT where VC_2 structure is formed, the frequencies of both oscillation modes alter, which suggests that the shape change of the vortex core structure such as the expansion of the core observed in VC_2 structure results in the change of oscillation frequency. More importantly, the drastic change of the FFT power spectra is witnessed around H_x = 15 mT where the dimensional change of the vortex core structure occurs. For 1D vortex core structures, VC_1 and VC_2 structures (H_x < 15 mT), there are only two distinct modes denoted by F_0^{1D} and F_1^{1D} with large and small powers. When the 1D vortex core structure is transformed into the 2D vortex core structure (H_x > 15 mT) and the VC_3 structure is established, various oscillation modes over a wide range of frequencies from MHz to sub-GHz appear. The F_0^{1D} and F_1^{1D} modes are split into five modes, denoted by F_0^{2D}, F_1^{2D}, F_2^{2D}, F_3^{2D}, and F_4^{2D} (Figure 4b). It is noted that intensities of F_2^{2D}, F_3^{2D}, and F_4^{2D} are relatively small compared to those of F_0^{2D}, and F_1^{2D}.

The modes of 1D and 2D vortex core structures are schematically illustrated in

Figures 4c-4e, which were confirmed by calculating inverse FFT corresponding to each oscillation mode (See Supplementary Figures 4, 5, Supplementary Notes 3 and 4). For the 1D vortex core structure (Figure 4c, Supplementary Figure 4 and Supplementary Note 3), mode F_0^{1D} corresponds to the gyrotropic motion of the vortex core structure, which is uniformly excited in the thickness direction without any node. Mode F_1^{1D} still corresponds to the gyrotropic motion of the vortex core structure, but in this case, at the centre of the vortex core structure in the thickness direction, the gyrotropic motion is not excited due to the node formed at the centre of the vortex core structure. That is, modes F_0^{1D} and F_1^{1D} are the zeroth- and first-order gyrotropic modes of vortex core structures, respectively. The modes F_0^{2D}, F_1^{2D}, and F_2^{2D} of 2D vortex core structures (Figures 4d, Supplementary Figure 5, and Supplementary Note 4) correspond to the gyrotropic motions of vortex cores on the top and bottom surfaces as well as the lateral motion of the domain wall. Similar to the modes of the 1D vortex core structure, mode F_0^{2D} corresponds to dynamic motion without a node, and mode F_1^{2D} represents dynamic motion including a node at the centre of the domain wall.

Additionally, it is found that the mode F_2^{2D} includes two nodes. Namely, the modes F_0^{2D}, F_1^{2D}, and F_2^{2D} are the zeroth-, first-, and second-order oscillation modes of the 2D vortex core structure, respectively. The modes F_3^{2D}, and F_4^{2D} correspond to the modes where the spin-wave propagates along the domain wall while the gyrotropic motions of vortex cores occur on the top and bottom surfaces. The spin-waves in modes F_3^{2D} and F_4^{2D} have different oscillation phases from each other. In mode F_3^{2D}, the vortex cores on the top surface shows the counter-clockwise (CCW) gyrotropic motion while the vortex cores on the bottom surface shows CW gyrotropic motion. In contrast, in mode F_4^{2D}, both vortex cores on the top and bottom surfaces show CW gyrotropic motion (See Figure 4e and Supplementary Note 4). The superposition of multiple oscillation modes is reflected by the flexure oscillation of the VC_3 structure including noticeable motion change observed in the experiment. The results in Figure 4 support that the oscillation properties of vortex core structures such as eigenfrequency, the number of oscillation modes, and the range of oscillation frequency, which are important features for developing vortex-based nano-oscillator, can be easily tuned by manipulating the shape and dimension of vortex core structure within a single magnetic

disk.

In summary, we demonstrate that the oscillation modes of vortex core structures can be controlled over the wide range of frequencies from MHz to sub-GHz by manipulating the shape and dimension of the vortex core structure within a single ferromagnetic disk. The observed various oscillation modes of the vortex core structure can be electrically excited by spin-transfer torque[13,52] and detected by magnetoresistance effects[13]. Moreover, the oscillation modes with sub-GHz frequency can be selectively excited based on the constructive/destructive interference phenomena, and therefore can be implemented into nano-devices. Our findings provide a fundamental understanding of the oscillation nature of spin structures and its dependency on the shape and dimension of spin structures, which would be essential information for the development of nano-oscillator and also bio-inspired devices utilizing the oscillation.

Methods

Sample fabrication.

The electrode of Ti (5 nm)/Au (50 nm) was fabricated on a 100 nm thick X-ray transparent silicon-nitride (Si_3N_4) membrane to apply an oersted field. On the electrode, Py circular disk was deposited using the dc sputtering. The circular disk of a diameter $D = 3\ \mu$m, and a thickness h = 100 nm was patterned by electron-beam lithography and lift-off processing.

X-ray imaging and time-resolved measurement.

The magnetization components in a Py circular disk were directly observed by utilizing full-field magnetic transmission X-ray microscopy (MTXM) at XM-1 beamline 6.1.2 the Advanced Light Source (ALS).[1] Out-of-plane magnetic components were imaged at the Fe L_3 X-ray absorption edge (708 eV). To image out-of-plane magnetic components, samples mounted with respect to the X-ray propagation direction. The MTXM contrasts represent a projection of out-of-plane magnetic components along the thickness direction. The images were normalized by an image with opposite photon helicity to enhance the MTXM contrasts.

The time-resolved measurement for X-ray imaging of dynamic behaviour of vortex core structures was performed by utilizing the stroboscopic pump-probe technique at two-bunch mode of the ALS where X-ray is injected with the frequency of 3.33MHz. We injected the Gaussian pulse of the amplitude V_{pp} = 2V and pulse width of 1.12 ns in Au electrodes. The injected pulse generates an oersted field pulse of the amplitude of 1 mT and a pulse width of 1.12 ns along −x-axis to excite the dynamic motion of vortex core structures in a Py

circular disk. By tuning the delay time between pump (field pulse) and probe (X-ray pulse), the time-resolved MTXM images are measured.

Micromagnetic simulation.

To specify the detailed magnetization configurations of spin structures and its dynamics, we carried out the micromagnetic simulation by using mumax[3] code[45] that can solve numerically the Landau-Lifshitz-Gilbert (LLG) equation: $\partial \mathbf{M}/\partial t = -\gamma_0(\mathbf{M}\times\mathbf{H}_{\text{eff}}) + (\alpha/|\mathbf{M}|)(\mathbf{M}\times\partial\mathbf{M}/\partial t)$ with the local magnetization vector $\mathbf{M}$, the gyromagnetic ratio γ_0, the effective field $\mathbf{H}_{\text{eff}}$, and the phenomenological damping constant α.[53,54] We employed a Py circular disk of a diameter D = 3 μm and a thickness h = 100 nm with the mesh size of 4 × 4 × 4 nm^3, which has exactly same dimension with the disk measured in our experiments. We used the typical material parameters of Py, i.e., saturation magnetization M_s = 800 kA/m, exchange stiffness A_{ex} = 13 pJ/m, and damping constant α = 0.01. To excite the dynamic motion of vortex core structure, we applied Gaussian field pulses with the amplitude of 1 mT and the pulse width of 1.12 ns in $-x$-axis.

Capturing position and area of vortex core structures in MTXM images.

To analyse the dynamics of spin structures quantitatively, MTXM contrasts were processed by Gaussian fitting. After Gaussian fitting, we normalized the MTXM contrasts. For the 1D vortex core structures (H_x = 0, and 12 mT), the area of the vortex core structure was defined as the area where the normalized MTXM contrast is smaller than 0.2. The position of the vortex core structure was determined as the centre of mass of the area of the

vortex core structure. For the 2D vortex core structure (H_x = 24 mT), we captured the position of the 2D vortex core structure, the minimum value of MTXM contrasts.

Fast Fourier Transformation (FFT).

In experiments, we obtained frequency spectra for the 1D and 2D vortex core structures by performing fast Fourier transformation (FFT) of x-position of the VC_1 (Supplementary Figure 3), and the shifted area of VC_3 structures (Figure 3c). To specify the oscillation mode of vortex core structures depending on the shape and dimension, by utilizing micromagnetic simulation, we applied the additional in-plane magnetic field with an amplitude of 1 mT to shift the vortex core structures from the initial position under static in-plane field H_x in the x-axis and turned off the additional magnetic field. We obtained frequency spectra with the frequency resolution of 10 MHz by performing FFT of the oscillation of magnetization vector at each discrete cell with varying H_x.

Data availability. The data that support the findings of this study are available from the corresponding author upon reasonable request.

References

1. Liu, G. *et al.* A charge-density-wave oscillator based on an integrated tantalum disulfide–boron nitride–graphene device operating at room temperature. *Nature Nanotechnology* **11**, 845-850, doi:10.1038/nnano.2016.108 (2016).

2. Zhu, C. *et al.* Light-Tunable 1T-TaS2 Charge-Density-Wave Oscillators. *ACS Nano* **12**, 11203-11210, doi:10.1021/acsnano.8b05756 (2018).

3. Zong, A. *et al.* Ultrafast manipulation of mirror domain walls in a charge density wave. *Science Advances* **4**, eaau5501, doi:10.1126/sciadv.aau5501.

4. Doiron-Leyraud, N. *et al.* Quantum oscillations and the Fermi surface in an underdoped high-Tc superconductor. *Nature* **447**, 565-568, doi:10.1038/nature05872 (2007).

5. Goteti, U. S., Zaluzhnyy, I. A., Ramanathan, S., Dynes, R. C. & Frano, A. Low-temperature emergent neuromorphic networks with correlated oxide devices. *Proceedings of the National Academy of Sciences* **118**, e2103934118, doi:10.1073/pnas.2103934118 (2021).

6. Kim, Y.-J., Jung, H., Han, S. W. & Kwon, O.-H. Ultrafast Electron Microscopy Visualizes Acoustic Vibrations of Plasmonic Nanorods at the Interfaces. *Matter* **1**, 481-495, doi:https://doi.org/10.1016/j.matt.2019.03.004 (2019).

7. Sie, E. J. *et al.* An ultrafast symmetry switch in a Weyl semimetal. *Nature* **565**, 61-66, doi:10.1038/s41586-018-0809-4 (2019).

8. Choe, S. B. *et al.* Vortex Core-Driven Magnetization Dynamics. *Science* **304**, 420, doi:10.1126/science.1095068 (2004).

9. Yu, Y.-S. *et al.* Resonant amplification of vortex-core oscillations by coherent magnetic-field pulses. *Scientific Reports* **3**, 1301, doi:10.1038/srep01301 (2013).

10. Satywali, B. *et al.* Microwave resonances of magnetic skyrmions in thin film multilayers. *Nature Communications* **12**, 1909, doi:10.1038/s41467-021-22220-1 (2021).

11. Dussaux, A. *et al.* Large microwave generation from current-driven magnetic vortex oscillators in magnetic tunnel junctions. *Nature Communications* **1**, 8, doi:10.1038/ncomms1006 (2010).

12. Yoo, M.-W. *et al.* Pattern generation and symbolic dynamics in a nanocontact vortex oscillator. *Nature Communications* **11**, 601, doi:10.1038/s41467-020-14328-7 (2020).

13. Pribiag, V. S. *et al.* Magnetic vortex oscillator driven by d.c. spin-polarized current. *Nature Physics* **3**, 498-503, doi:10.1038/nphys619 (2007).

14. Marković, D. & Grollier, J. Quantum neuromorphic computing. *Applied Physics Letters* **117**, 150501, doi:10.1063/5.0020014 (2020).

15. Liu, H. *et al.* A Tantalum Disulfide Charge-Density-Wave Stochastic Artificial Neuron for Emulating Neural Statistical Properties. *Nano Letters* **21**, 3465-3472, doi:10.1021/acs.nanolett.1c00108 (2021).

16. Romera, M. *et al.* Vowel recognition with four coupled spin-torque nano-oscillators. *Nature* **563**, 230-234, doi:10.1038/s41586-018-0632-y (2018).

17. Torrejon, J. *et al.* Neuromorphic computing with nanoscale spintronic oscillators. *Nature* **547**, 428-431, doi:10.1038/nature23011 (2017).

18. Grollier, J. *et al.* Neuromorphic spintronics. *Nature Electronics* **3**, 360-370, doi:10.1038/s41928-019-0360-9 (2020).

19. Jung, H. *et al.* Logic Operations Based on Magnetic-Vortex-State Networks. *ACS Nano* **6**, 3712-3717, doi:10.1021/nn3000143 (2012).

20. Ma, F., Zhou, Y., Braun, H. B. & Lew, W. S. Skyrmion-Based Dynamic Magnonic Crystal. *Nano Letters* **15**, 4029-4036, doi:10.1021/acs.nanolett.5b00996 (2015).

21. Hubert, A. & Schäfer, R. *Magnetic Domains: The Analysis of Magnetic Microstructures*. (Springer, 1998).

22. Guslienko, K. Y. *et al.* Eigenfrequencies of vortex state excitations in magnetic submicron-size disks. *Journal of Applied Physics* **91**, 8037-8039, doi:10.1063/1.1450816 (2002).

23. Metlov, K. L. & Guslienko, K. Y. Stability of magnetic vortex in soft magnetic nano-sized circular cylinder. *Journal of Magnetism and Magnetic Materials* **242-245**, 1015-1017, doi:https://doi.org/10.1016/S0304-8853(01)01360-9 (2002).

24. Van Waeyenberge, B. *et al.* Magnetic vortex core reversal by excitation with short bursts of an alternating field. *Nature* **444**, 461-464, doi:10.1038/nature05240 (2006).

25. Kammerer, M. *et al.* Magnetic vortex core reversal by excitation of spin waves. *Nature Communications* **2**, 279, doi:10.1038/ncomms1277 (2011).

26. Cowburn, R. P. Change of direction. *Nature Materials* **6**, 255-256, doi:10.1038/nmat1877 (2007).

27. Yamada, K. *et al.* Electrical switching of the vortex core in a magnetic disk. *Nature Materials* **6**, 270-273, doi:10.1038/nmat1867 (2007).

28. Ivanov, B. A. & Zaspel, C. E. High Frequency Modes in Vortex-State Nanomagnets. *Physical Review Letters* **94**, 027205, doi:10.1103/PhysRevLett.94.027205 (2005).

29. Novosad, V. *et al.* Magnetic vortex resonance in patterned ferromagnetic dots. *Physical Review B* **72**, 024455, doi:10.1103/PhysRevB.72.024455 (2005).

30. Finizio, S. *et al.* Control of the gyration dynamics of magnetic vortices by the magnetoelastic effect. *Physical Review B* **96**, 054438, doi:10.1103/PhysRevB.96.054438 (2017).

31. Filianina, M. *et al.* Piezo-electrical control of gyration dynamics of magnetic vortices. *Applied Physics Letters* **115**, 062404, doi:10.1063/1.5110169 (2019).

32. Lee, K.-S. & Kim, S.-K. Two circular-rotational eigenmodes and their giant resonance asymmetry in vortex gyrotropic motions in soft magnetic nanodots. *Physical Review B* **78**, 014405, doi:10.1103/PhysRevB.78.014405 (2008).

33. Ding, J., Kakazei, G. N., Liu, X. M., Guslienko, K. Y. & Adeyeye, A. O. Intensity inversion of vortex gyrotropic modes in thick ferromagnetic nanodots. *Applied Physics Letters* **104**, 192405, doi:10.1063/1.4878617 (2014).

34. Han, H.-S., Lee, S., Jung, D.-H., Kang, M. & Lee, K. S. Chirality-dependent asymmetric vortex core structures in a harmonic excitation mode. *Applied Physics Letters* **117**, 042401, doi:10.1063/5.0010926 (2020).

35. Lv, G., Zhang, H., Cao, X., Gao, F. & Liu, Y. Micromagnetic simulations of magnetic normal modes in elliptical nanomagnets with a vortex state. *Applied Physics Letters* **103**, 252404, doi:10.1063/1.4850537 (2013).

36. Noske, M. *et al.* Three-dimensional Character of the Magnetization Dynamics in Magnetic Vortex Structures: Hybridization of Flexure Gyromodes with Spin Waves. *Physical Review Letters* **117**, 037208, doi:10.1103/PhysRevLett.117.037208 (2016).

37. Guslienko, K. Y., Kakazei, G. N., Ding, J., Liu, X. M. & Adeyeye, A. O. Giant moving vortex mass in thick magnetic nanodots. *Scientific Reports* **5**, 13881, doi:10.1038/srep13881 (2015).

38. Yoo, M.-W., Lee, J.-H. & Kim, S.-K. Excited eigenmodes in magnetic vortex states of soft magnetic half-spheres and spherical caps. *Journal of Applied Physics* **116**, 223902, doi:10.1063/1.4903815 (2014).

39. Boust, F. & Vukadinovic, N. Micromagnetic simulations of vortex-state excitations in soft magnetic nanostructures. *Physical Review B* **70**, 172408, doi:10.1103/PhysRevB.70.172408 (2004).

40. Yan, M., Hertel, R. & Schneider, C. M. Calculations of three-dimensional magnetic normal modes in mesoscopic permalloy prisms with vortex structure. *Physical Review B* **76**, 094407, doi:10.1103/PhysRevB.76.094407 (2007).

41. Ding, J., Kakazei, G. N., Liu, X., Guslienko, K. Y. & Adeyeye, A. O. Higher order vortex gyrotropic modes in circular ferromagnetic nanodots. *Scientific Reports* **4**, 4796, doi:10.1038/srep04796 (2014).

42. Buchanan, K. S. *et al.* Magnetic-field tunability of the vortex translational mode in micron-sized permalloy ellipses: Experiment and micromagnetic modeling. *Physical Review B* **74**, 064404, doi:10.1103/PhysRevB.74.064404 (2006).

43. Yakata, S., Tanaka, T., Kiseki, K., Matsuyama, K. & Kimura, T. Wide range tuning of resonant frequency for a vortex core in a regular triangle magnet. *Scientific Reports* **3**, 3567, doi:10.1038/srep03567 (2013).

44. Fischer, P. *et al.* Soft X-ray microscopy of nanomagnetism. *Materials Today* **9**, 26-33, doi:https://doi.org/10.1016/S1369-7021(05)71335-3 (2006).

45. Vansteenkiste, A. *et al.* The design and verification of MuMax3. *AIP Advances* **4**, 107133, doi:10.1063/1.4899186 (2014).

46. Han, H.-S. *et al.* Topology-dependent stability of vortex-antivortex structures. *Applied Physics Letters* **118**, 212407, doi:10.1063/5.0045593 (2021).

47. Mayr, S. *et al.* Spin-Wave Emission from Vortex Cores under Static Magnetic Bias Fields. *Nano Letters* **21**, 1584-1590, doi:10.1021/acs.nanolett.0c03740 (2021).

48. Im, M.-Y. *et al.* Dynamics of the Bloch point in an asymmetric permalloy disk. *Nature Communications* **10**, 593, doi:10.1038/s41467-019-08327-6 (2019).

49. Graf, J., Pfeifer, H., Marquardt, F. & Viola Kusminskiy, S. Cavity optomagnonics with magnetic textures: Coupling a magnetic vortex to light. *Physical Review B* **98**, 241406, doi:10.1103/PhysRevB.98.241406 (2018).

50. Cheynis, F. *et al.* Controlled Switching of N\'eel Caps in Flux-Closure Magnetic Dots. *Physical Review Letters* **102**, 107201, doi:10.1103/PhysRevLett.102.107201 (2009).

51. Masseboeuf, A. *et al.* Dimensionality Crossover in Magnetism: From Domain Walls (2D) to Vortices (1D). *Physical Review Letters* **104**, 127204, doi:10.1103/PhysRevLett.104.127204 (2010).

52. Yu, X. W. *et al.* Images of a Spin-Torque-Driven Magnetic Nano-Oscillator. *Physical Review Letters* **106**, 167202, doi:10.1103/PhysRevLett.106.167202 (2011).

53. Gilbert, T. L. A Lagrangian formulation of the gyromagnetic equation of the magnetization field. *Physical Review* **100**, 1243 (1955).

54. Landau, L. D. & Lifshitz, E. M. On the theory of the dispersion of magnetic permeability in ferromagnetic bodies. *Phys. Z. Sowjetunion* **8**, 153-164 (1955).

Acknowledgement

Works at the ALS were supported by the U.S. Department of Energy (DE-AC02-05CH11231). J.-I.H. was supported by the National Research Foundation of Korea (NRF) grant funded by Korea government (MSIT) (2020R1A2C2005932). K.-S.L. was supported by the NRF grant funded by Korea government (MSIT) (2019R1A2C2002996, 2019K1A3A7A09033400, and 2020M3F3A2A03082987), and was funded by the 2019 Research Fund (1.190038.01) of UNIST (Ulsan National Institute of Science and Technology). M.-Y.I. acknowledges support by Lawrence Berkeley National Laboratory through the Laboratory Directed Research and Development (LDRD) Program.

Author Contributions

H.-S. H., M.-Y. I., K.-S. L. designed and planned the research. H.-S. H., S. L., M.-S. J., N. K., M. K., H.-J. O., Y.-S. Y., M.-Y. I, K.-S. L performed the experiments. S. L., M.-S.J., Y.-S. Y., W. C., J.-I. H. prepared the samples. H.-S. H., M.-Y. I., K.-S. L. analysed data. K.-S. L., H.-S. H. carried out the micromagnetic simulations. H.-S. H., M.-Y. I., K.-S. L. prepared the manuscript, which incorporates critical input from all authors.

Competing financial interests

The authors declare no competing financial interests.

Figures

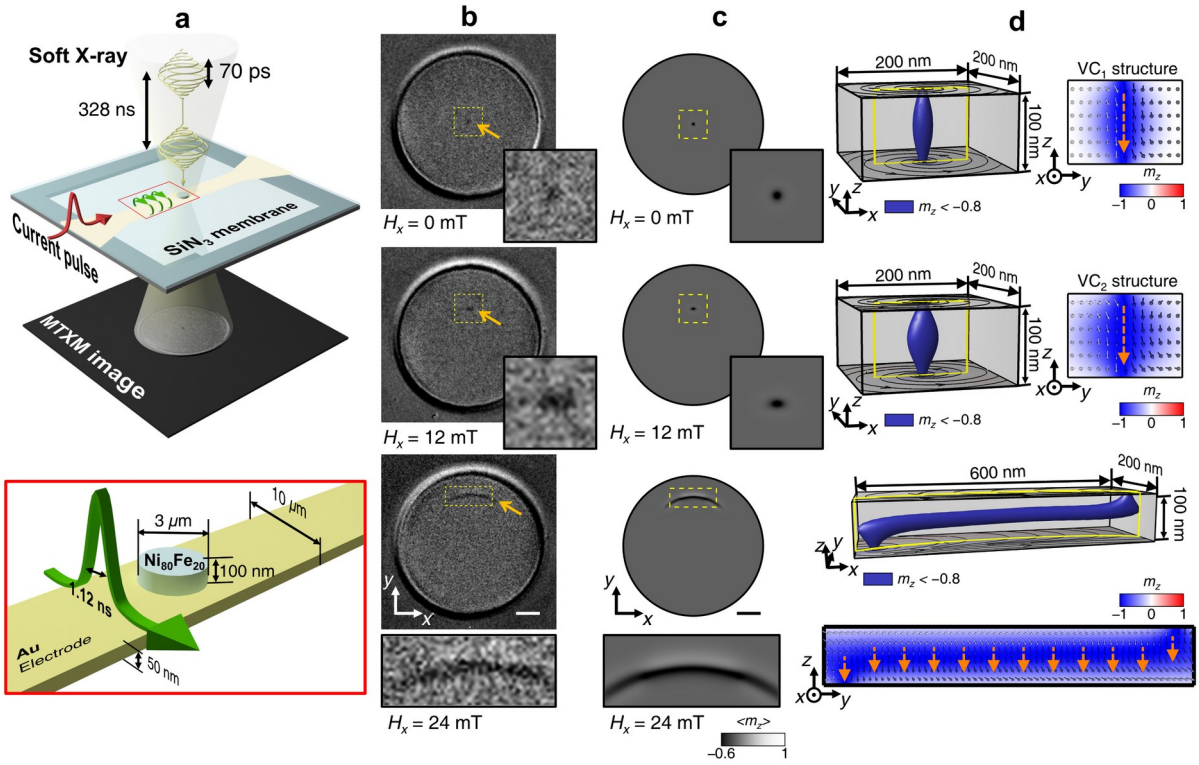

Figure 1 | Controlling the shape and dimension of the vortex core structure. a-c, (**a**) Schematic of the experimental setup of the magnetic transmission X-ray microscopy (MTXM). The zoomed image in the red box is inserted with the permalloy (Py, $Ni_{80}Fe_{20}$) circular disk of diameter 3 μm and thickness 100 nm on 50 nm-thick Au electrode. (**b**) Out-of-plane magnetic structures observed in a Permalloy (Py, $Ni_{80}Fe_{20}$) circular disk of diameter 3 μm and thickness 100 nm by magnetic transmission X-ray microscopy (MTXM) with varying the magnetic field H_x in the x-axis (scale bar: 500 nm). Zoomed images of the out-of-plane magnetic structures are inserted. The black and white contrasts indicate the downward and upward out-of-plane magnetic components, respectively. The vortex core structures are indicated by orange arrows. (**c**) Simulated magnetization images corresponding to MTXM images (scale bar: 500 nm). (**d**) The internal magnetization configurations of vortex core structures marked by the yellow dashed box in Fig. 1c. The magnetization configurations representing the cross-section of vortex core structures are visualized.

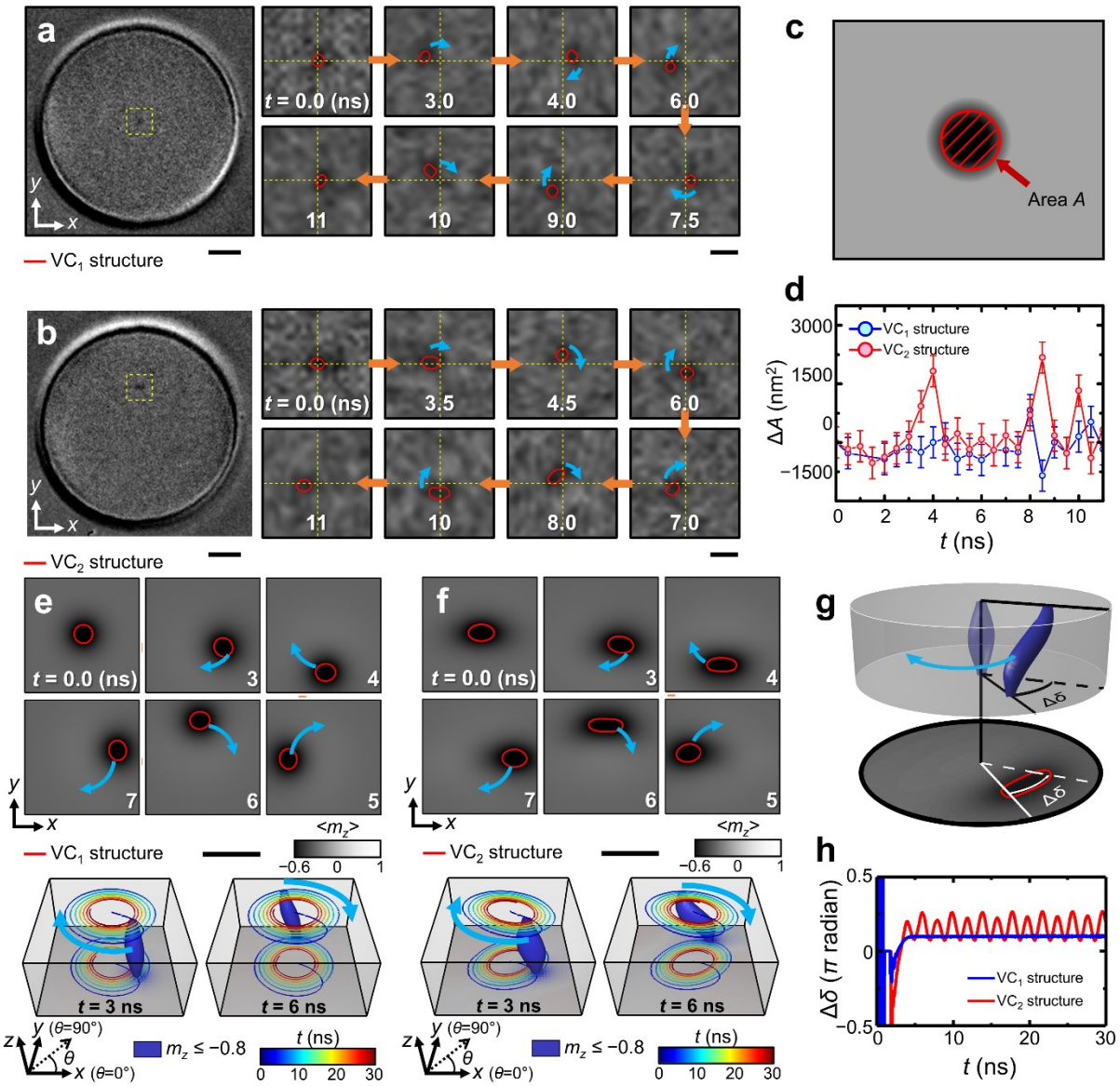

Figure 2 | The dynamics of 1D vortex core structures. a-h, Time-resolved X-ray images of the dynamic motions of VC_1 (**a**) and VC_2 (**b**) structures, respectively (scale bars in representative MTXM images and zoomed images are 500 nm and 100 nm, respectively). (**c**) The area A inside the red closed curve indicates the vortex core structure. (**d**) The variation of the A as a function of the time. The blue and red lines indicate the variation of A of VC_1 and VC_2 structures. The series of simulated magnetic images for the dynamic motions of VC_1 (**e**) and VC_2 (**f**) structures (above) in micromagnetic simulations (scale bar: 100 nm) and the snapshots of their internal magnetization structures captured at t = 3 and 6 ns with trajectory curves (below) of vortex cores on the top and bottom surfaces of the disk. (**g**) The schematic illustration of the X-ray imaging of the vortex core structure, and the phase difference between vortex cores on the top and bottom surfaces $\Delta\delta$. (**h**) The variation of $\Delta\delta$ during the dynamic motions of vortex core structures. The blue and red lines indicate $\Delta\delta$ of VC_1 and VC_2 structures, respectively.

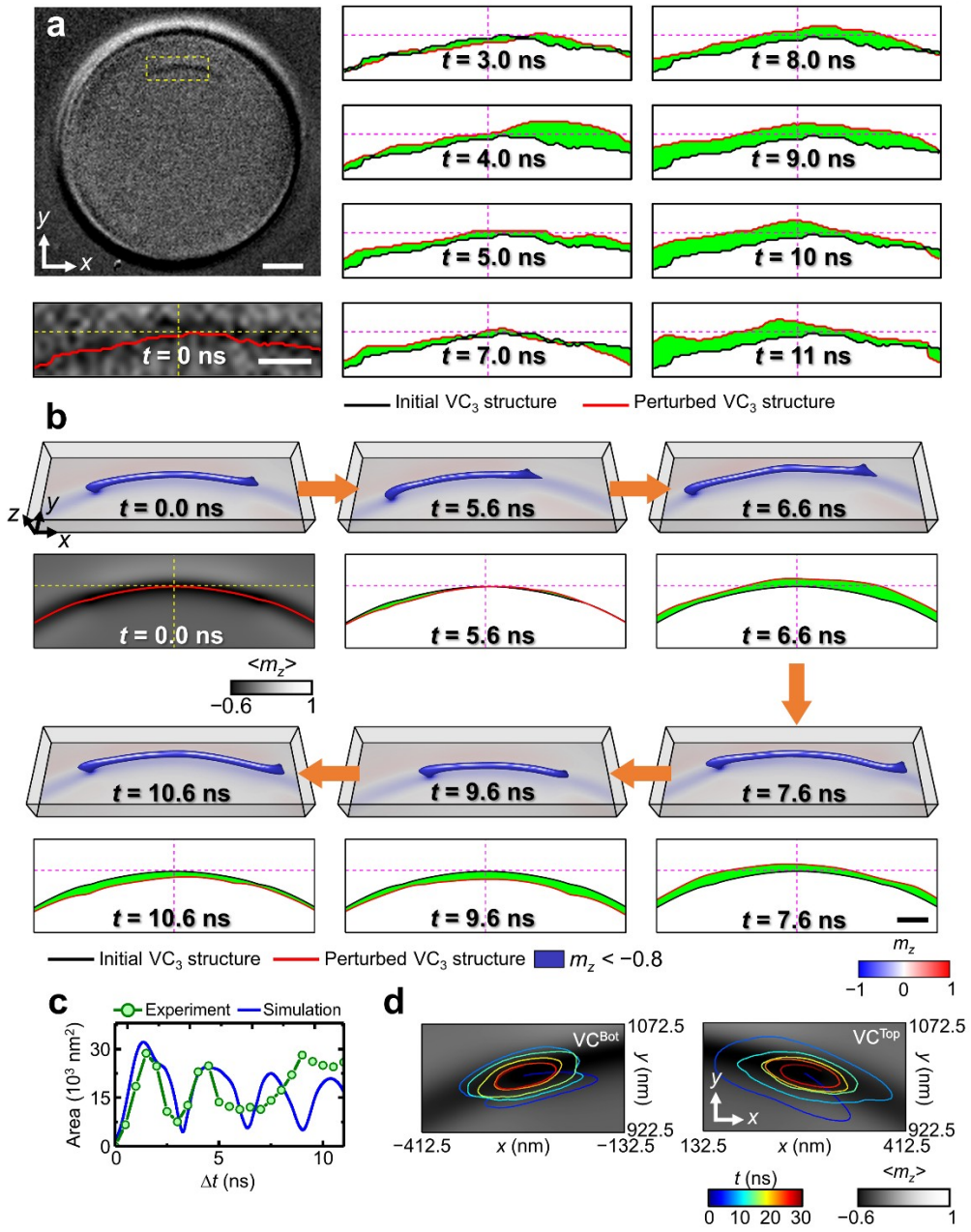

Figure 3 | The dynamics of the 2D vortex core structure. a-d, (**a**) The series of magnetic images for the dynamic motion of the VC_3 structure taken by time-resolved MTXM. The black line indicates the initial position of the VC_3 structure at t = 0 ns. (scale bars in the representative MTXM images and zoomed images: 500 nm and 300 nm, respectively). (**b**) The snapshot images of the 3D magnetization configurations (above) of VC_3 structures and the core structures (below), which were obtained from micromagnetic simulation during the dynamic motion (scale bar: 100 nm). The red lines in Figs. 3a and 3b indicate the perturbed position of the VC_3 structure. The area between those two lines is filled in green colour. (**c**) The variations of the green-coloured area obtained from the experiment (green line) and simulation (blue line) data in Figs. 3a and 3b which show the perturbation of the dynamic

motions of the VC_3 structure, quantitatively. (**d**) The trajectory curves of vortex cores on the top and bottom surfaces of the disk obtained from the micromagnetic simulation.

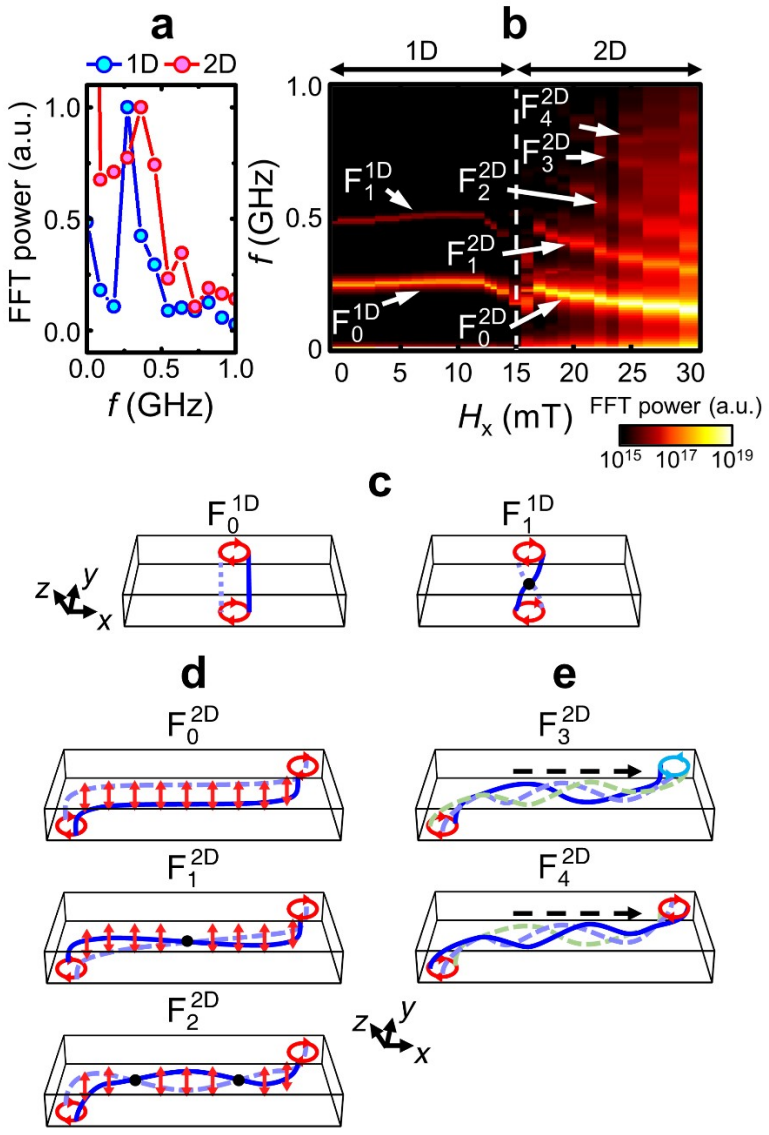

Figure 4 | The oscillation modes of vortex core structures formed with varying the in-plane magnetic field. a-d, (**a**) The fast Fourier transformation (FFT) power spectra for the 1D and 2D vortex core structures obtained from the MTXM measurements. The red and blue lines indicate the normalized FFT power spectrum of VC_1 and VC_3 structures, respectively. (**b**) FFT power spectra for vortex core structures as function of H_x taken from micromagnetic simulation. The white dashed line indicates H_x = 15 mT where the dimensional change of the vortex core structure from 1D to 2D occurs. The schematic illustrations of the zeroth- and higher-order modes of 1D (F_0^{1D}, and F_1^{1D}) (**c**) and 2D (F_0^{2D}, F_1^{2D}, and F_2^{2D}) (**d**) vortex core structures. (**e**) The modes F_3^{2D}, and F_4^{2D} where spin-wave propagates along the domain wall of the 2D vortex core structure are schematically illustrated. The black dashed line indicates the spin-wave propagation direction. The clockwise and counter-clockwise gyrotropic motions of vortex cores on the top and bottom surfaces are denoted by the red and light blue arrows, respectively. The black dashed line indicates the spin-wave propagation direction.